Multimodal and multiscale correlative elemental imaging: From whole tissues down to organelles

Stéphane Roudeau, Asuncion Carmona, Richard Ortega

Multimodal and multiscale correlative elemental imaging: from whole tissues down to organelles

Stéphane Roudeau[1], Asuncion Carmona[1], Richard Ortega[1]

Address

[1] Univ. Bordeaux, CNRS, LP2I, UMR 5797, F-33170 Gradignan, France

Corresponding author: Ortega, Richard (richard.ortega@u-bordeaux.fr)

Abstract

Chemical elements, especially metals, play very specific roles in the life sciences. The implementation of correlative imaging methods, of elements on the one hand and of molecules or biological structures on the other hand, is the subject of recent developments. The most commonly used spectro-imaging techniques for metals are synchrotron-induced X-ray fluorescence, mass spectrometry and fluorescence imaging of metal molecular sensors. These imaging methods can be correlated with a wide variety of other analytical techniques used for structural imaging (e.g., electron microscopy), small molecule imaging (e.g., molecular mass spectrometry) or protein imaging (e.g., fluorescence microscopy). The resulting correlative imaging is developed at different scales, from biological tissue to the subcellular level. The fields of application are varied, with some major research topics, the role of metals in the aetiology of neurodegenerative diseases and the use of metals for medical imaging or cancer treatment.

Keywords

Imaging, Correlative, Element, Metal, Tissue, Brain, Cell, Neuron, Organelle, Synchrotron, X-ray fluorescence, Mass spectrometry, Molecular imaging, SIMS, Laser ablation.

Abbreviations

BSE, backscattered electron imaging; CLEM, correlative light-electron microscopy; DAPNe, direct analyte-probed nanoextraction; DESI, desorption electrospray ionization; FTIR, Fourier-transform infrared spectroscopy; HD-MIBI = high-definition multiplex ion beam imaging; HIM-SIMS, helium ion microscope secondary ion mass spectrometer; IF, immunofluorescence ; IMC, imaging mass cytometry; LA-ICP, laser ablation inductively coupled plasma; LC, liquid chromatography; MS, mass spectrometry; MSI, mass spectrometry imaging ; O-PTIR, optical photothermal infrared imaging; PCI, phase contrast imaging; PIXE, particle induced X-ray emission; qBEI, quantitative backscattered electron imaging; SIM, structured illumination microscopy; SIMS, secondary ion MS; SiR, silicon rhodamine; SN, substantia nigra; SR, synchrotron radiation; SR-FITR, synchrotron-based Fourier transform infrared spectro-microscopy; STED, stimulated emission depletion microscopy; SXRF, synchrotron X-ray fluorescence; SXT, soft X-ray tomography; TEM, transmission electron microscopy; TH, tyrosine hydroxylase; TOF, time-of-flight; XANES, X-ray absorption near edge structure; Zn-STIMO = simultaneously tracking Zn^{2+} in multiple organelles.

Introduction

'*Nature loves to hide*'. These elegant words, written by Heraclitus of Ephesus about 2,500 years ago, can be interpreted in many ways. As researchers, we may recognize the great game of hide-and-seek that Nature loves to play. The development of new analytical tools has always been a key parameter to answer the many questions that arise in Biology. Multiple and complementary analytical techniques are needed to unravel the mechanisms underlying complex biological processes and their pathological dysfunctions. This is particularly true for the study of metals in Biology. The information about the sole localization of the metal in tissues or cells is generally not enough to understand the molecular mechanisms of action. Ideally, metal localization should be compared to the structural organization of the cell or tissue, and/or to the localization of biomolecules (proteins, nucleic acids, lipids…).

The main techniques for imaging metals in biological samples are based either on X-ray emission spectrometry e.g. particle induced X-ray emission (PIXE) and synchrotron X-ray fluorescence (SXRF), on mass spectrometry (MS) e.g. laser ablation inductively coupled plasma MS (LA-ICP-MS) and secondary ion MS (SIMS), or on fluorescence microscopy of metal specific fluorescent probes (Tables 1 & 2). The characteristics of these imaging techniques in terms of sensitivity, spatial resolution and quantitative analysis as well as their capabilities to address biological questions have been exhaustively reviewed [1-5]. On the other hand, the imaging of biological molecules can be achieved by a variety of instruments available to characterize the biological tissues (Tables 1 & 2), from optical and fluorescence microscopy (e.g. histological staining, immuno-staining), electron microscopy, infrared microscopy, and mass spectrometry for organic compounds analysis.

Another important requirement to understand the effects of metals on biological processes is that different scales of observation are needed, from the tissue level down to the subcellular level. Depending on the nature of the studied samples, tissue sections or single cells, the sample preparation may differ drastically (Tables 1 & 2). In this article, we will review the last two years research dedicated to the imaging of chemical elements and their correlation with biological molecules or structures. We will first review the state-of-the-art for correlative imaging of biological tissues, as a continuation and update of the review article from Perry et al. [6] in this journal, and secondly we will present the correlative imaging at the subcellular level.

Correlative elemental imaging at the biological tissue level

Correlative imaging enables the characterization of distinct microscopic features in *ex vivo* tissues and comparison with element localization (Table 1). The fields of application are mainly for the understanding of the homeostatic dysfunction of metals in various pathologies (cancer, tuberculosis, neurodegenerative diseases...), using human tissues or animal models. A second topic in development is the use of metals or halogenated compounds (Br, I) as markers for biological molecules such as antibodies.

Correlation of elemental distribution with tissue structures

The simplest yet most informative way to correlate chemical element maps with the structure of a biological sample is simply to perform serial sections of the sample and histological staining. One of the sections is stained for histology. Another section, not stained, is deposited on a support adapted to the chosen chemical imaging method for comparison of chemical element localization and tissue

organization. This comparison allowed, for example, to define the distribution of platinum in tumors collected from patients treated with a platinum-based anticancer drug. Histological sections were compared to time-of flight (TOF) LA-ICP-MS images. The results of this study show strong heterogeneity of platinum distribution in tumors [7]. It is also possible to obtain information on the structural organization through electron microscopy. This is the case of bone tissue whose mineralization can be characterized by quantitative backscattered electron imaging (qBEI) [8], allowing the histological identification of bone structures and compare with chemical element maps obtained by SXRF. This methodology was applied to study the potential toxicity of Gd contrast imaging molecules to the bone structure. Both SXRF and qBEI were performed on the same tissue sections, embedded with poly(methyl methacrylate) (PMMA), offering a direct unbiased correlative imaging. However, this protocol is limited to the study of tightly bound elements to the biological matrix, which is the case for Gd and Ca in bone tissues.

Correlation of elemental distribution with proteins labelled with antibodies

Similarly to histological staining, immunohistochemical labelling is a simple and very informative alternative for correlating element distributions with well identified regions of biological tissues. For example, metal analysis was performed by micro-PIXE, micro-SXRF and micro- X-ray absorption near edge structure (XANES) to determine element distributions and Fe oxidation state in the substantia nigra (SN) pars compacta and pars reticulata identified by tyrosine hydroxylase (TH) immunohistochemistry [9]. This study explains how to prepare adjacent facing sections of biological tissue, mirroring each other, which allows the analysis of two sections by two different imaging methods but on the two faces of the same specimen. Using a similar methodology, SXRF was combined to immuno-fluorescence (IF) microscopy on adjacent facing sections to determine the metal content of Cu,Zn superoxide dismutase aggregates [10]. In another example, histological staining and immunohistochemistry were applied to identify atherosclerotic plaques and to compare with the distribution of metal-based contrast agents at different scales, by LA-ICP-MS and SXRF [11].

A recent development of micro-PIXE analysis enables to perform the correlative imaging on the same tissue section by detecting simultaneously chemical elements and proteins labelled with a Ni-tagged antibody. Using this original strategy, micro-PIXE element mapping was conducted to quantify Fe in Parkinson's disease brains within specific cell types (neurons, oligodendrocytes, microglia, astroglia) identified by Ni-enhanced immunocytochemical detection [12]. This strategy is similar to the one developed for imaging mass cytometry (IMC) which uses metal-tags to image proteins by high resolution LA-ICP-MS offering a very powerful tool for imaging up to 42 antigenic markers on a single section of tissue [13]. IMC was recently combined to another LA-ICP-MS setup to compare the immuno-histology with the distribution of endogenous metals (Mg, Cu, Zn) in sections of a 3D model of lung adenocarcinoma cells [14]. Also with the goal of identifying proteins by immunolabeling with atoms that can be detected by chemical element imaging, another study proposes the synthesis of an iodinated derivative of an immunoglobulin G complex conjugated to erythrosine B that can be detected by both SXRF and immunofluorescence [15]. This bimodal probe enabled to identify dopaminergic neurons in tissue sections from mice brains.

Correlation of elemental distribution with MSI

Mass spectrometry imaging (MSI) methods such as desorption electrospray ionization (DESI)-MSI are now widely used to locate low molecular weight molecules (e.g. metabolites, drugs...) at the scale of a

tissue or an organ. Correlating MSI with chemical element imaging would allow significant progresses in many research fields. In the already cited study of a 3D model of lung adenocarcinoma cells, IMC, LA-ICP-MS and DESI-MSI were performed respectively for protein-localization, chemical element imaging and imaging of metabolites (lactate, glutamine, citrate…) and other low molecular weight molecules (fatty acids, glutathione) [14]. In this example, the analyses were performed on distinct tissue sections prepared with protocols suited to each imaging technique. However, the challenge is to make the sample preparation compatible for applying MSI and elemental imaging on the same sample. The proof of concept of MSI followed by elemental chemical imaging has been recently provided [16]. Lung tissue sections from an animal model of tuberculosis were imaged first by DESI-MSI then by PIXE, on the same section, clearly showing a correlation at the 50-µm scale between specific lipids markers of tuberculosis and some chemical elements such as Fe. An alternative approach to MSI is liquid extraction surface analysis, where a discrete region of a sample is probed [17]. The combination of direct analyte-probed nanoextraction (DAPNe) and liquid chromatography (LC)-MS to identify lipids, and PIXE micro-analysis for element imaging, revealed an association between foamy macrophage regions and Fe accumulation in a rabbit model of tuberculosis. This study also enabled to compare the distribution at the tissue level of a Br-containing anti-tuberculosis drug, bedaquiline, that could be detected both by micro-PIXE and by DAPNe-LC-MS showing for both methods that the drug concentration was higher in the cellular rim.

Correlation of elemental distribution with FTIR

Fourier-transform infrared spectroscopy (FTIR) imaging is also very frequently used for the chemical imaging of biological macromolecules in tissue sections and provides key information on chemical changes during pathogenesis. When combined to elemental imaging, FTIR can contribute to elucidate pathological mechanisms involving metals. For example, synchrotron radiation (SR) µFTIR and SXRF were performed on the same areas of human brain sections from Alzheimer's (AD) disease patients [18]. SR-µFTIR enabled to locate and distinguish fibrillary and nonfibrillary amyloid plaques. SXRF revealed that the concentrations of Fe, Cu and Zn were higher in the amyloid plaques. Cu and Zn were co-located with the amyloid deposits while Fe was associated with the border of the plaques. Fe concentrations were found higher in fibrillary plaques than in nonfibrillary ones. In addition, XANES at Fe absorption edge revealed the presence of Fe(II) and Fe(III) in the amyloid deposits, with a decreased content of Fe(II) in fibrillary plaques vs non fibrillary ones. In another study, the development of a methodological workflow for the calculation of correlative coefficients between SXRF and FTIR images of full rat brains sections shows very interesting features (Figure 1). For example, a high correlation between phosphorous and aliphatic signals could be generally concluded and between Fe signals and tyrosine residues [19].

Correlation of elemental distribution with TEM

A recent development succeeded in correlating nano-SXRF imaging to transmission electron microscopy (TEM), a reference method for ultrastructural microscopy [20]. This new achievement was applied to rat brain tissues in an experimental model of Parkinson's disease. The mapping of trace metals using SXRF was performed on 500 nm- thick tissue sections, while TEM was performed on adjacent 80 nm-thin sections. Trace element concentrations could be quantified unambiguously in cellular organelles such as the nucleus, nucleolus or cytoplasm.

Correlative elemental imaging at organelle level

The elemental imaging of biological tissues generally uses thin or semi-thin sections, whereas subcellular imaging often starts from cell cultures as described in the next sections (Tables 1 & 2). It is also important to note the great heterogeneity of cellular sample preparation methods: cryofixation and freeze-drying, chemical fixation, fully cryogenic protocols, etc. No standard correlative technique stands out and the same is true for sample preparation protocols, each solution must be adapted to the question asked, with its own advantages and limitations.

Elemental imaging techniques used for correlative studies

Recent publications show a certain homogeneity in the techniques used for elemental imaging at the subcellular level. In correlative mode SXRF imaging is widely used, followed by SIMS and finally by an example of structured illumination microscopy (SIM) (Table 2). SXRF was employed to identify the organelles of manganese accumulation in parkinsonism, revealing Mn-rich nano-vesicles in the Golgi apparatus [21, 22]. Another example of SXRF application is the identification at high spatial resolution (pixel size 25-50 nm) of Fe/S-rich cytoplasmic granules in the SN of Parkinson's disease model in rats [20]. In a neuronal model of AD, Fe clusters detected by SXRF colocalized with amyloid β-sheet structures [23]. Correlative SXRF imaging has also been used to study uranium neurotoxicity with formation of cytoplasmic aggregates in dopaminergic cells [24], the distribution of elements (P, S, Cl, K, Ca) and metals (Fe, Zn) in the growth cones of developing neurons [25] and the mitochondrial localization of silver in hepatocytes exposed to silver nanoparticles [26]. Correlation at the molecular/macromolecular scale is now possible. SXRF nano-imaging beamlines reach resolutions of 30 nm, comparable to the resolutions of super-resolution optical microscopy techniques. This allowed the identification of copper and zinc associated with cytoskeletal proteins in dendritic spines [27]. Correlating the distribution of trace elements with the localization of organelles could ideally be done at the SXRF step. Thus, several publications report the development of rhenium or bromine-based organelle trackers (turn-on fluorescent probes) for SXRF imaging of mitochondria [28, 29]. Another approach is the construction and expression of fusion proteins with a lanthanide binding motif (europium, erbium). Cytosolic or membrane proteins tagged with lanthanide are then directly detectable by the X-ray fluorescence of these heteroatoms [30].

There are very few recent examples of correlative 3D SXRF imaging at the subcellular scale, probably due to the difficulties of implementing these techniques, sample preparation constraints, acquisition time and data processing. Nevertheless, two publications present the state of the art and directions for 3D correlative SXRF imaging of eukaryotic cells. Conesa and colleagues performed 3D mapping of the intracellular distribution of an anticancer drug (iridium metallodrug) with a step size of 70 nm and precisely demonstrated its localization in the mitochondria of breast cancer cells (Figure 2) [31]. Another 3D study focused on subcellular imaging and local quantification of elements (P, S, Cl, K, Ca, Mn, Fe, Zn) in entire macrophage [32]. These two studies were conducted in fully cryogenic mode. Finally, SXRF tomography was also successfully used to image a membrane protein on the surface of *E. coli* [30].

Nano-SIMS imaging offers a spatial resolution of approximately 50-100 nm and allows elemental and isotopic analysis. Nano-SIMS imaging has been used in 'dual' correlation with correlative light-electron microscopy (CLEM) to analyse the isotopic composition (^{14}N, ^{12}C, ^{31}P, ^{32}S) of organelles in HeLa cells [33]. In another study, NanoSIMS was correlated with TEM to demonstrate the subcellular distribution of a platinum-based drugs in the nucleus and nucleoli of human colon cancer cell lines [34], and HeLa

cells [35] with 30 nm lateral resolution. NanoSIMS was also used in correlation with TEM, as well as helium ion microscope secondary ion mass spectrometer (HIM-SIMS) in correlation with backscattered electron (BSE), for high-resolution intracellular Fe imaging in macrophages, with a spatial resolution down to 20 nm for HIM-SIMS showing Fe accumulation within mitochondria and vacuole-like organelles [36]. Finally, apart from SXRF and Nano-SIMS techniques, there is an example of correlative imaging of the labile zinc pool at super resolution based on structured illumination microscopy (SIM) with a specific turn-on Zn^{2+} fluorescent probe designed for the simultaneous tracking of Zn in multiple organelles (Zn-STIMO) [37].

Organelle imaging techniques used for correlative studies

The techniques used for organelle imaging are divided into three main categories: fluorescence light microscopy, SR-based methods and electron microscopy. Through the diversity of these approaches, all organelles can be located, as well as proteins in some cases (Table 2). In fluorescence light microscopy (epifluorescence, confocal, or super-resolution), correlation is investigated by the use of organelle-specific trackers of the subcellular compartments: nucleus [22, 24], lysosomes and mitochondrial network [28-30, 33], or of multiple organelles [37]. Organelle localization can also be achieved by expression of fluorescent fusion proteins (e.g. GFP, RFP tag) with targeting sequence to the Golgi apparatus, endosomes, lysosomes, or endoplasmic reticulum [22, 24]]. Direct labelling of cellular proteins is also possible and has been used in stimulated emission depletion (STED) super-resolution microscopy for actin and tubulin labelling with silicon-rhodamine (SiR) fluorophores [25, 27, 38]. By using STED microscopy and SXRF on the same sample with a similar spatial resolution, below 40 nm, it was possible to discriminate between thin cellular structures such as microtubules in cultured neurons that could not be separated by confocal microscopy [38].

SR methods can be used to reveal the 3D cellular ultrastructure by cryo soft X-ray tomography (cryo-SXT) which is based on the measurement of the local intracellular density. Organelles are segmented based on these density differences. The volume resolution is excellent (50 nm) and the technique requires a fully cryogenic protocol to maintain frozen hydrated cells at cryogenic temperature in a near-native state [31] (Figure 2). Another 3D SR-based technique is X-ray holographic nanotomography. Used in correlation with SXRF in entire frozen-hydrated macrophage cells (resolution 20 nm for SXRF, 40 nm for holograms), it allows to measure the local mass density and to precisely quantify the molar concentration of major and minor elements taking into account X-ray self-absorption [32]. SXRF imaging has been correlated with phase contrast imaging (PCI) to locate dense subcellular structures [27, 39] or with SR optical photothermal infrared (O-PTIR) imaging to characterize amyloid structures [23].

A correlative method of choice for the ultrastructural study remains TEM. It has been used alone or in combination (CLEM) as a complement to 2D elemental analyses conducted in SXRF [20, 26, 31, 33]. The preparation of TEM samples remains restrictive (chemical fixation, contrast agents, substitution, sections, etc.) and disturbs the distribution of diffusible elements, which may compromise the generalization of its use in correlation with elemental analysis on the same section. Finally, correlations between elements and very fine subcellular structures can also be established in NanoSIMS using antibodies tagged with specific isotopes (^{19}F, ^{81}Br, ^{127}I, ^{197}Au). This high-definition multiplex ion beam imaging (HD-MIBI) approach enabled to correlate Pt distribution from the chemotherapeutic agent cisplatin to subnuclear structures, at 30 nm spatial resolution in 3D [35].

Perspectives

Correlative imaging of metals and biological molecules and/or structures allows to allocate specific activities to certain regions of a biological tissue or cell. Studies that will integrate multi-scale approaches in addition to multimodal imaging should provide a better understanding of the mechanisms of action of metals in biology. Regions of metal compartmentalization at the tissue level, for example in the brain, are often highlighted and constitute the first step before moving to a finer resolution to identify the subcellular or molecular actors of this compartmentation. A multimodal characterization, not only bimodal, is desirable to obtain the most exhaustive information possible but is often hampered by the incompatibility of preparation methods for each analysis technique. Work is needed today to improve the compatibility of imaging techniques. Another possible improvement will be to perform multimodal imaging, with the same instrument, to identify and localize both the metal and the biological molecules of interest. This objective seems to be achievable by several approaches, for example SXRF or SIMS imaging, by labelling biological molecules with exogenous atoms while maintaining the localization of endogenous elements.

Declaration of competing interest

Declarations of interest: none.

Acknowledgements

The authors acknowledge financial support from CNRS (Centre National de la Recherche Scientifique) through the MITI (Mission pour les initiatives transverses et interdisciplinaires) program ‘Osez l’Interdisciplinarité.’

Table 1. Correlative elemental imaging studies of tissues (2019-2022)

Application	Sample	Elemental imaging techniques and analytes	Correlative techniques and analytes	Spatial resolution	Sample preparation	Reference
Cancer chemotherapy with metallodrugs	Human brain tumors	LA-ICP-TOFMS : Mg, P, S, Ca, Fe, Cu, Zn, Gd, Pt	Optical microscopy (histology) : hematoxylin and eosin staining	LA-ICP-TOFMS : 10 µm Optical microscopy ≈ 2 µm	Paraffin-embedded tumor sections (5 µm)	[7]
Gadolinium toxicity	Human bones	SXRF: Gd, Ca	qBEI: tissue mineralization	SXRF : 20 µm qBEI : 1 µm	PMMA-embedded tissue sections (3 µm)	[8]
Metal dyshomeostasis in Parkinson's disease	Mice brain	PIXE, SXRF : P, S, Cl, K, Ca, Mn, Fe, Cu, Zn XANES: Fe(II)/Fe(III)	Immuno-histochemistry : tyrosine hydroxylase	PIXE: 2 µm SXRF and XAS: 4 µm	Fresh frozen tissue sections (20-50 µm)	[9]
Metal dyshomeostasis in Parkinson's disease	Human brain	SXRF: K, P, S, Fe, Cu, Zn	IF: superoxide dismutase; α-synuclein X-ray ptychography: tissue structure (aggregates)	SXRF : 100 nm Immuno-fluorescence: 2 µm X-ray ptychography: 13.5 nm	Fresh frozen tissue sections (20 µm)	[10]
Contrast agent for atherosclerosis diagnostic	Rabbit aortic arch	SXRF: P, S, Ca, Fe, Gd LA-ICP-MS: Fe, Eu, Gd	Immuno-histochemistry: smooth muscle cells, actin, macrophages.	SXRF: 0.6 x 0.8 μm^2 LA-ICP-MS: 20 µm	Formalin fixation, paraffin embedded sections (5 µm and 20 µm for elemental imaging).	[11]
Fe dyshomeostasis in Parkinson's disease	Human brain	PIXE : Fe	Immuno-µ-PIXE : Ni-tagged antibodies for protein markers of brain cells	2D PIXE: 2 µm Immuno-µ-PIXE: 2 µm	Chemically fixed sections (2 µm)	[12]
Metal dyshomeostasis in carcinogenesis	3D cell cultures, lung adenocarcinoma	LA-ICP-MS : Mg, Cu, Zn	DESI : metabolites, fatty acids, glutathione. IMC: metal-tag antibodies targeting protein markers for tumors.	LA-ICP-MS : 6 µm DESI-MS : 30 µm IMC : 1 µm	Chemically fixed sections (10 µm)	[14]
Analytical development	Mice brain	SXRF: iodine	Immunofluorescence: tyrosine hydroxylase	SXRF: not mentioned Immuno-SXRF: not mentioned	Chemically fixed sections (30 µm)	[15]
Metal dyshomeostasis in tuberculosis	Rabbit lung tissue	PIXE : S, Fe, Zn	DESI : lipids	PIXE : 2 µm DESI : 75 µm	Fresh frozen tissue sections (10 µm)	[16]
Metal dyshomeostasis in tuberculosis	Rabbit lung tissue	PIXE: Cl, K, Fe, Br	DAPNe-LCMS: lipids, bedaquiline (anti-tuberculosis drug)	PIXE : 2 µm DAPNe-LCMS : 5 µm	Cryosections (10 µm)	[17]
Metal dyshomeostasis in Alzheimer's disease	Human brain	SXRF: Fe, Cu, Zn XANES: Fe(II)/Fe(III)	SR-FTIR: β sheet aggregation	SXRF: 90 nm XANES: 0.4 x 0.9 μm^2 SR-FTIR: 6 µm	Formalin fixed brain tissues. Frozen sections (8 µm).	[18]
Analytical development	Rat brain	SXRF: P S, Cl, K, Ca, Fe, Cu, Zn	FTIR: chemical bounds	SXRF: 100 x 200 μm^2 FTIR: 100 µm	Fresh-frozen cryosections (20 µm)	[19]
Metal dyshomeostasis in Parkinson's disease	Rat brain	SXRF: P, S, Ca, Fe	TEM: nucleus, nucleolus, cytoplasmic granules	SXRF : 25-50 nm TEM: 1.5 nm	Freezing, resin embedding, adjacent sections	[20]

Table 2. Correlative elemental imaging studies of subcellular organelles (2019-2022)

Application	Sample	Elemental imaging technique	Correlative technique	Organelles or subcellular analytes	2D/3D, spatial resolution (pixel size)	Sample preparation	Reference
Parkinsonism and accumulation of Mn in the Golgi apparatus	HeLa cells	SXRF	Epifluorescence	Golgi apparatus, endoplasmic reticulum, nucleus, GFP-Mn-transport-protein	2D SXRF : 50-500 nm	SXRF: cryofixation, +/- freeze-drying (air vs cryo)	[22]
Imaging Mn storage in Golgi apparatus	HEK293T cells	SXRF	Epifluorescence	Golgi apparatus, nucleus, Mn-sensor	2D SXRF : 300 nm	cryofixation, freeze-drying	[21]
3D intracellular imaging and quantification of iridium-based drug	MCF7 line (breast cancer cells)	SXRF tomography	SXT, TEM	Nucleus, dense vesicles, lipid droplets, vacuoles, mitochondria, cell membrane, acidic organelles	3D SXRF : 70 nm SXT : 50 nm	TEM: fixation, resin embedding, thin sections 70 nm, U, Pb Epifluorence, Cryo SXT Cryo SXRF: cryofixation (fully cryogenic))	[31]
Correlative imaging of metals and cytoskeleton proteins in dendrites and spines	Primary rat hippocampal neurons	SXRF	Confocal, STED, PCI	Dendritic spines, actin, tubulin	2D SXRF : 40 nm STED : 25 nm	STED: live imaging SXRF: cryofixation, freeze drying	[27]
3D subcellular imaging and quantification of elements in entire cells	Macrophage cells	SXRF	X-ray holographic nanotomography	Vacuoles, nucleus, cytoplasm, Golgi apparatus, endoplasmic reticulum, nuclear membrane	3D SXRF : 120 nm Holograms : 40 nm	SXRF, X-ray holographic nanotomography: cryofixation (fully cryogenic)	[32]
Element colocalization with amyloid β-sheet, lipids	Alzheimer's disease-like neurons	SXRF	O-PTIR	Fibrillary forms of amyloid-β proteins, lipids	3D SXRF : 200-500 nm O-PTIR: 300-500 nm	Fixation, freeze drying	[23]
Nano-imaging of elements in Parkinson's disease model	Dopaminergic neurons from rat substantia nigra	SXRF	TEM	Nucleus, nucleolus, cytoplasm, cytoplasmic granules	2D SXRF : 25-50 nm TEM : 1.5 nm	Freezing, resin embedding, adjacent sections	[20]
Cytoplasmic aggregation of uranium	SH-SY5Y cells (dopaminergic)	SXRF	Epifluorescence	Lysosomes, endosomes, nucleus, specific protein	2D SXRF : 300 nm)	Cryofixation, freeze-drying	[24]
Super-resolution imaging of zinc in multiple organelles	HeLa cells	SIM, Zn-STIMO	SIM, Zn-STIMO	Mitochondria, lysososmes, endoplasmic reticulum	2D, 3D SIM and Zn-STIMO : 100 nm	Live imaging	[37]

Isotopic composition of cellular components	HeLa cells	NanoSIMS	CLEM	Mitochondria, dense granules, euchromatin, heterochromatin	2D Epifuorescence : 320 nm TEM : 22 nm NanoSIMS : 164 nm	Freeze substitution, resin embedding, sections	[33]
Subcellular distribution of platinum-based drug and of its isotope labeled moieties	Human colon cancer cell lines	NanoSIMS	TEM	Nucleus, nucleolus, mitochondria, endosmes, lysosomes.	2D NanoSIMS : 80 nm	High-pressure freezing, resin embedding, adjacent sections	[34]
Subcellular localization of proteins and molecules using heteroatoms and isotopes	HeLa cells	NanoSIMS	NanoSIMS, HD-MIBI	Nucleolus, transcriptionally active/silent chromatin, centromeres, subnuclear structures, mitochondria	2D, 3D NanoSIMS : 30 nm (lateral), 5 nm (axial)	NanoSIMS compatible protocol with permeabilisation	[35]
Mitochondria trackers for SXRF imaging and optical fluorescence microscopy	A549 (epithelial human lung carcinoma cells)	SXRF	Epifluorescence	Mitochondria	2D SXRF : 500 nm	SXRF: fixation (PFA), air drying	[28]
Subcellular imaging and quantification of silver after AgNP exposure	HepG2 cells (hepatocytes)	SXRF	TEM	Mitochondria, nucleus	2D SXRF : 50 nm	Fixation (PFA, glutaraldehyde), OsO4, resin embedding, sections	[26]
Imaging lanthanide tagged proteins using SXRF	*E. coli*	SXRF, tomography	SXRF, tomography	Proteins (cytosolic vs membrane)	2D/3D SXRF : 40 nm	bacteria embedded in NaCl micro crystals	[30]
Mapping of chemical element in developing neurons	Primary rat hippocampal neurons	SXRF	Confocal, STED	Actin, tubulin	2D, SXRF 85-200 nm (SXRF), STED : 40 nm	cryofixation, freeze-drying	[25, 38]
Mitochondria trackers for SXRF imaging and optical fluorescence microscopy	CCD-19Lu cells (fibroblasts), HeLa cells	SXRF	Confocal	Mitochondria	2D SXRF : 300 nm	SXRF: fixation (PFA), air drying	[29]

Figure 1

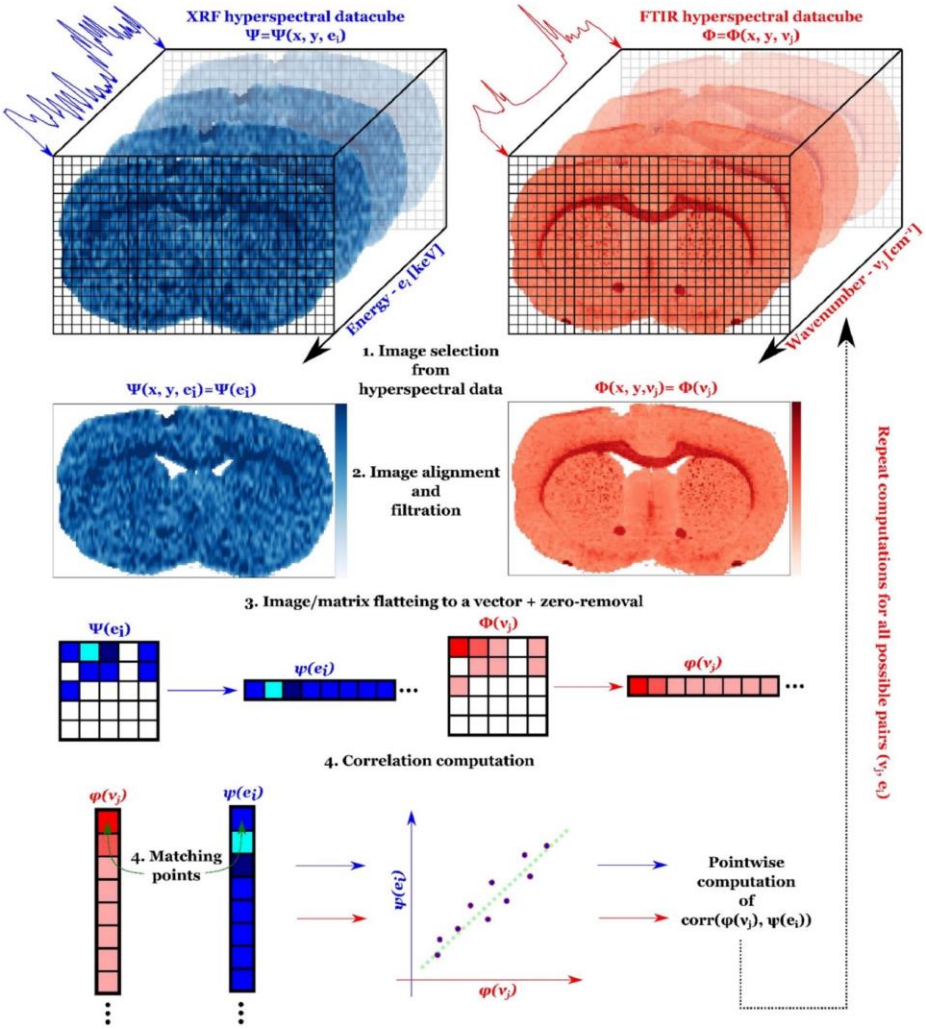

Layout of the procedure for *in situ* quantification of correlation between molecular components and chemical elements in the brain tissue. 2D correlograms are obtained by computing SXRF and FTIR hyperspectral datacubes, based on whole sample area [19]. Reproduced with permission.

Figure 2. Unambiguous intracellular localization and quantification of a potent iridium anticancer compound by correlative 3D cryo X-Ray imaging. Conesa et al. performed cryo SXT and cryo SXRF tomography in MCF7 cells to precisely locate an iridium-based compound in the mitochondrial network. (a) SXT image is overlaid with epifluorescence signal from mitochondria (green) and acidic organelles (red). (b) Iridium distribution and quantification on same region. (c) mitochondria (green) and iridium signal (purple). (d) reconstructed slices from the cryo-SXT and the SXRF tomography (yellow square) and iridium density. (e) and (f) are slices across mitochondria confirming the location of iridium. (g) 3D rendering after segmentation of organelles (cryo SXT). The iridium signal (SXRF tomography) found in mitochondria is represented as a yellow mesh [31]. Reproduced with permission.

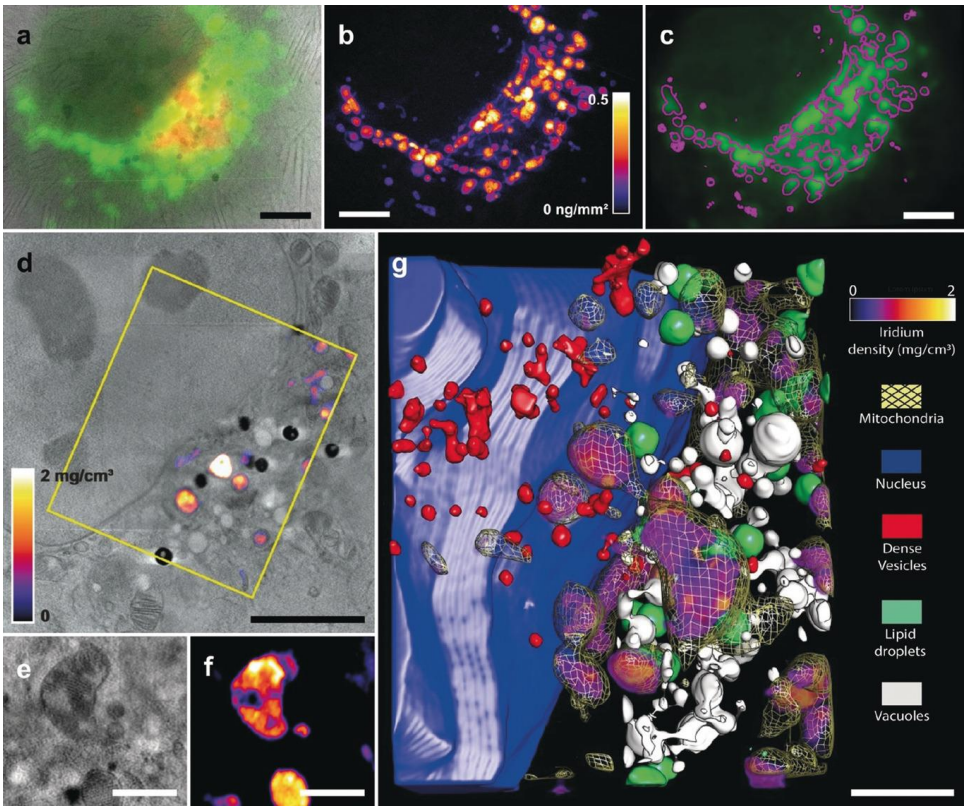

References

Papers of particular interest, published within the period of review,

have been highlighted as:

* of special interest

* * of outstanding interest

1. da Cunha MML, Trepout S, Messaoudi C, Wu T-D Di, Ortega R, Guerquin-Kern J-LL, Marco S: **Overview of chemical imaging methods to address biological questions**. *Micron* 2016, **84**:23–36.

2. Ackerman CM, Lee S, Chang CJ: **Analytical methods for imaging metals in biology: from transition metal metabolism to transition metal signaling**. *Anal Chem* 2017, **89**:22-41.

3. New EJ, Wimmer VC, Hare DJ: **Promises and pitfalls of metal imaging in biology**. *Cell Chem Biol* 2018, **25**:7-18.

4. Decelle J, Veronesi G, Gallet B, Stryhanyuk H, Benettoni P, Schmidt M, Tucoulou R, Passarelli M, Bohic S, Clode P, Musat N: **Subcellular Chemical Imaging: New Avenues in Cell Biology.** *Trends Cell Biol* 2020, **30**:173-188.

5. Zee DZ, MacRenaris KW, O'Halloran TV: **Quantitative imaging approaches to understanding biological processing of metal ions.** *Curr Opin Chem Biol* 2022, **69**:102152.

6. Perry WJ, Weiss A, Van de Plas R, Spraggins JM, Caprioli RM, Skaar EP: **Integrated molecular imaging technologies for investigation of metals in biological systems: A brief review**. *Curr Opin Chem Biol* 2020, **55**:127-135.

7. Theiner S, Schweikert A, Haberler C, Peyrl A, Koellensperger G: **Laser ablation-ICP-TOFMS imaging of germ cell tumors of patients undergoing platinum-based chemotherapy**. *Metallomics* 2020, **12**:1246-1252.

8. Turyanskaya A, Rauwolf M, Pichler V, Simon R, Burghammer M, Fox OJL, Sawhney K, Hofstaetter JG, Roschger A, Roschger P, Wobrauschek P, Streli C: **Detection and imaging of gadolinium accumulation in human bone tissue by micro- and submicro-XRF**. *Sci Rep* 2020, **10**:6301.

9. Carmona A, Roudeau S, Perrin L, Carcenac C, Vantelon D, Savasta M, Ortega R: **Mapping chemical elements and iron oxidation states in the substantia nigra of 6-hydroxydopamine lesioned rats using correlative immunohistochemistry with proton and synchrotron micro-analysis.** *Front Neurosci* 2019, **13**:1014.

10. Genoud S, Jones MWM, Trist BG, Deng J, Chen S, Hare DJ, Double KL: **Simultaneous structural and elemental nano-imaging of human brain tissue**. *Chem Sci* 2020, **11**:8919-8927.

11. Uca YO, Hallmann D, Hesse B, Seim C, Stolzenburg N, Pietsch H, Schnorr J, Taupitz M: **Microdistribution of magnetic resonance imaging contrast agents in atherosclerotic plaques determined by LA-ICP-MS and SR-µXRF imaging**. Mol Imaging Biol 2021, **23**:382-393.

12. Friedrich I, Reimann K, Jankuhn S, Kirilina E, Stieler J, Sonntag M, Meijer J, Weiskopf N, Reinert T, Arendt T, Morawski M: **Cell specific quantitative iron mapping on brain slices by immuno-µPIXE in healthy elderly and Parkinson's disease**. *Acta Neuropathol Commun* 2021, **9**:47.

13. Kakade VR, Weiss M, Cantley LG: **Using imaging mass cytometry to define cell identities and interactions in human tissues.** *Front Physiol* 2021, **12**:817181.

14. Flint LE, Hamm G, Ready JD, Ling S, Duckett CJ, Cross NA, Cole LM, Smith DP, Goodwin RJA, Clench MR: **Characterization of an aggregated three-dimensional cell culture model by multimodal mass spectrometry imaging**. *Anal Chem* 2020, **92**:12538-12547.

15. Yan M, Zuo T, Zhang J, Wang Y, Zhu Y, Wang L, Zhou Y, Sun Y: **A bimodal probe for fluorescence and synchrotron X-ray fluorescence imaging of dopaminergic neurons in the brain.** *Chem Commun (Camb)* 2022, **58**:713-715.

16.* de Jesus JM, Costa C, Burton A, Palitsin V, Webb R, Taylor A, Nikula C, Dexter A, Kaya F, Chambers M, Dartois V, Goodwin RJA, Bunch J, Bailey MJ: **Correlative imaging of trace elements and intact molecular species in a single-tissue sample at the 50 µm scale**. *Anal Chem* 2021, **93**:13450-13458.

The authors describe how to correlate DESI mass spectrometry imaging and PIXE elemental imaging on the same sample to gain insight from organic compounds information and trace metal distribution in lung tissue from a rabbit model of tuberculosis.

17. Lewis HM, Costa C, Dartois V, Kaya F, Chambers M, de Jesus J, Palitsin V, Webb R, Bailey MJ: **Colocation of lipids, drugs, and metal biomarkers using spatially resolved lipidomics with elemental mapping**. *Anal Chem* 2022, **94**:11798-11806.

18.** Álvarez-Marimon E, Castillo-Michel H, Reyes-Herrera J, Seira J, Aso E, Carmona M, Ferrer I, Cladera J, Benseny-Cases N: **Synchrotron X-ray fluorescence and FTIR signatures for amyloid fibrillary and nonfibrillary plaques.** *ACS Chem Neurosci* 2021, **12**:1961-1971.

The authors use SXRF for element imaging, XANES for Fe oxidation state and FTIR to characterize the aggregation state of amyloid plaques in Alzheimer's disease brains. The results show different iron concentration and speciation in fibrillary vs nonfibrillary structures of the amyloid plaques.

19. Surowka AD, Czyzycki M, Ziomber-Lisiak A, Migliori A, Szczerbowska-Boruchowska M: **On 2D-FTIR-XRF microscopy - A step forward correlative tissue studies by infrared and hard X-ray radiation.** Ultramicroscopy 2022, **232**:113408.

20. Lemelle L, Simionovici A, Colin P, Knott G, Bohic S, Cloetens P, Schneider BL: **Nano-imaging trace elements at organelle levels in substantia nigra overexpressing α-synuclein to model Parkinson's disease**. *Commun Biol* 2020, **3**:1–10.

21. Das S, Carmona A, Khatua K, Porcaro F, Somogyi A, Ortega R, Datta A: **Manganese Mapping Using a Fluorescent Mn2+ Sensor and Nanosynchrotron X-ray Fluorescence Reveals the Role of the Golgi Apparatus as a Manganese Storage Site**. *Inorg Chem* 2019, **58**:13724–13732.

22. Carmona A, Zogzas CE, Roudeau S, Porcaro F, Garrevoet J, Spiers KM, Salomé M, Cloetens P, Mukhopadhyay S, Ortega R: **SLC30A10 Mutation Involved in Parkinsonism Results in Manganese Accumulation within Nanovesicles of the Golgi Apparatus.** *ACS Chem Neurosci* 2019, **10**:599–609.

23. * Gustavsson N, Paulus A, Martinsson I, Engdahl A, Medjoubi K, Klementiev K, Somogyi A, Deierborg T, Borondics F, Gouras GK, et al.: **Correlative optical photothermal infrared and X-ray fluorescence for chemical imaging of trace elements and relevant molecular structures directly in neurons**. *Light Sci Appl* 2021, **10**.

24. Carmona A, Porcaro F, Somogyi A, Roudeau S, Domart F, Medjoubi K, Aubert M, Isnard H,

Nonell A, Rincel A, et al.: **Cytoplasmic aggregation of uranium in human dopaminergic cells after continuous exposure to soluble uranyl at non-cytotoxic concentrations**. *Neurotoxicology* 2021, **82**:35–44.

25. Carmona A, Chen S, Domart F, Choquet D, Ortega R: **Imaging the structural organization of chemical elements in growth cones of developing hippocampal neurons**. *Metallomics* 2022, **14**.

26. Tardillo Suárez V, Gallet B, Chevallet M, Jouneau PH, Tucoulou R, Veronesi G, Deniaud A: **Correlative transmission electron microscopy and high-resolution hard X-ray fluorescence microscopy of cell sections to measure trace element concentrations at the organelle level**. *J Struct Biol* 2021, **213**.

27. * Domart F, Cloetens P, Roudeau S, Carmona A, Verdier E, Choquet D, Ortega R: **Correlating sted and synchrotron xrf nano-imaging unveils cosegregation of metals and cytoskeleton proteins in dendrites**. *Elife* 2020, **9**:1–18.

The authors describe the correlation of two high spatial resolution techniques (STED and nano-SXRF, <40 nm) to reveal Cu and Zn cosegregation with actin and tubulin in dendrites from primary neurons.

28. Schanne G, Henry L, Ong HC, Somogyi A, Medjoubi K, Delsuc N, Policar C, García F, Bertrand HC: **Rhenium carbonyl complexes bearing methylated triphenylphosphonium cations as antibody-free mitochondria trackers for X-ray fluorescence imaging**. *Inorg Chem Front* 2021, **8**:3905–3915.

29. Nagarajan S, Poyer F, Fourmois L, Naud-Martin D, Medjoubi K, Somogyi A, Schanne G, Henry L, Delsuc N, Policar C, et al.: **Cellular Detection of a Mitochondria Targeted Brominated Vinyl Triphenylamine Optical Probe (TP−Br) by X-Ray Fluorescence Microscopy**. *Chem – A Eur J* 2022, **28**.

30. Victor TW, O'Toole KH, Easthon LM, Ge M, Smith RJ, Huang X, Yan H, Chu YS, Chen S, Gursoy D, et al.: **Lanthanide-Binding Tags for 3D X-ray Imaging of Proteins in Cells at Nanoscale Resolution**. *J Am Chem Soc* 2020, **142**:2145–2149.

31. ** Conesa JJ, Carrasco AC, Rodríguez-Fanjul V, Yang Y, Carrascosa JL, Cloetens P, Pereiro E, Pizarro AM: **Unambiguous Intracellular Localization and Quantification of a Potent Iridium Anticancer Compound by Correlative 3D Cryo X-Ray Imaging**. *Angew Chemie - Int Ed* 2020, **59**:1270–1278.

The authors present the combination of X-ray fluorescence and soft X-ray tomography for 3D imaging and quantification of chemical elements in organelles in cryogenic mode, on a whole cell and with a spatial resolution of about 50 nm.

32. ** Gramaccioni C, Yang Y, Pacureanu A, Vigano N, Procopio A, Valenti P, Rosa L, Berlutti F, Bohic S, Cloetens P: **Cryo-nanoimaging of Single Human Macrophage Cells: 3D Structural and Chemical Quantification**. *Anal Chem* 2020, **92**:4814–4819.

This work describes the use of X-ray fluorescence and X-ray holographic nanotomography with the same synchrotron beamline for 3D imaging and quantifying elements at the subcellular level in frozen hydrated macrophage.

33. Lange F, Agüi-Gonzalez P, Riedel D, Phan NTN, Jakobs S, Rizzoli SO: **Correlative fluorescence microscopy, transmission electron microscopy and secondary ion mass spectrometry (CLEM-SIMS) for cellular imaging**. *PLoS One* 2021, **16**:1–17.

34. Legin AA, Schintlmeister A, Sommerfeld NS, Eckhard M, Theiner S, Reipert S, Strohhofer D, Jakupec MA, Galanski M, Wagner M, et al.: **Nano-scale imaging of dual stable isotope labeled**

oxaliplatin in human colon cancer cells reveals the nucleolus as a putative node for therapeutic effect. *Nanoscale Adv* 2021, **3**:249–262.

35. ** Rovira-Clavé X, Jiang S, Bai Y, Zhu B, Barlow G, Bhate S, Coskun AF, Han G, Ho CMK, Hitzman C, et al.: **Subcellular localization of biomolecules and drug distribution by high-definition ion beam imaging**. *Nat Commun* 2021, **12**:1–18.

The authors employed specific isotope-tagged antibodies with nanoSIMS to map the subcellular localisation of proteins and molecules with 30 nm resolution.

36. Lovrić J, Najafinobar N, Kurczy ME, De Castro O, Biesemeier A, Von Sydow L, Klarqvist M, Wirtz T, Malmberg P: Correlative High-Resolution Imaging of Iron Uptake in Lung Macrophages. Anal Chem 2022.

37. Fang H, Geng S, Hao M, Chen Q, Liu M, Liu C, Tian Z, Wang C, Takebe T, Guan JL, et al.: **Simultaneous Zn2+ tracking in multiple organelles using super-resolution morphology-correlated organelle identification in living cells**. *Nat Commun* 2021, **12**:1–5.

38. Ortega R, Roudeau S, Carmona A: **Correlative nano-imaging of metals and proteins in primary neurons by synchrotron X-ray fluorescence and STED super resolution microscopy: Experimental validation**. *J Neurosci Methods* 2022, **381**:109702.

39. Santos SP, Yang Y, Rosa MTG, Rodrigues MAA, De La Tour CB, Sommer S, Teixeira M, Carrondo MA, Cloetens P, Abreu IA, et al.: **The interplay between Mn and Fe in Deinococcus radiodurans triggers cellular protection during paraquat-induced oxidative stress**. *Sci Rep 2019*, **9**:1–12.